

Chemical Laser Systems Analysis

John R. Doughty*

Ben-Gurion University of the Negev, Beer-Sheva, Israel

This paper presents a means by which the chemical laser device weight can be minimized with respect to its performance and the device power minimized with respect to the target range. Chemical laser performance parameters such as the specific power and nozzle power flux are then used in conjunction with weight and propagation models to determine system effectiveness. A measure of merit is given by which systems can be contrasted. An illustrative example is included in which DF and Iodine laser systems are compared for an airborne scenario.

Nomenclature

A	= flow cross-sectional area (m^2)
AO	= adaptive optics
a_o	= aperture beam size (m)
B	= geometric weight factor (kg/m^2)
C	= fluid supply weight factor, dimensionless
C_n^2	= atmospheric structure constant ($\text{m}^{-2/3}$)
C_p	= specific heat at constant pressure ($\text{J}/\text{kg} - \text{K}$)
D	= aperture diameter (m)
E	= pressure recovery efficiency weight factor ($\text{m}^2 - s$)
F	= fixed weight constant (kg)
G	= Gaussian beam radius (m)
H	= altitude (m)
I	= intensity (W/cm^2)
K_i	= constants in Eq. (3); K_1 (kJ/kg), K_2 (m^2/kW)
k	= specific heat ratio, dimensionless
L_{TB}	= thermal blooming loss, dimensionless
M	= Mach number, dimensionless
M_i	= measure of merit ($\text{W}/\text{kg} - \text{cm}^2$)
N	= thermal distortion parameter, dimensionless
N_A	= number of actuators for a deformable mirror, dimensionless
n_o	= refractive index, dimensionless
n_i	= coefficient of index change with temperature (K^{-1})
n_x	= resonator extraction efficiency, dimensionless
P	= power (kW)
p	= pressure (Pa)
R	= range (m or km as specified)
R_g	= gas constant ($\text{J}/\text{kg} - \text{K}$)
r	= radius (m)
r_{CL}	= atmospheric correlation length (m)
r_F	= average mirror reflectivity, dimensionless
S	= specific power (kJ/kg)
SR	= Strehl ratio, dimensionless
s	= scattering coefficient (km^{-1})
T	= temperature (K)
T_A	= atmospheric transmission, dimensionless
t	= total laser device run time, including transients (s)
v_o	= average wind velocity (m/s)
W	= laser device system weight (kg)
w_s	= slew rate (rad/s)
Z	= system weight optimization parameter, Eq. (5)
α	= absorption coefficient (km^{-1})
β	= beam quality
Γ	= atmospheric extinction coefficient (km^{-1})

δ	= nozzle power flux (kW/m^2)
ε	= aperture linear obscuration ratio, dimensionless
θ	= single axis jitter standard deviation (rad)
λ	= wavelength (m)
ρ	= density (kg/m^3)
σ	= beam spread (rad)
Φ	= dilution ratio, dimensionless
ϕ	= rms wavefront error due to mirror surface figure (waves)
Ω	= $\sqrt{k[2/(k+1)]^{(k+1)/[2(k-1)]}}$, dimensionless

Subscripts

a	= aerosol
c	= cavity
D	= diffraction
E	= edge
I	= index
J	= pointing jitter
m	= maximum, molecular
P	= peak
S	= spot
t	= turbulent
v	= device outcoupled

Superscripts

n	= number of mirrors in beam train between the device and the final aperture
-----	---

Introduction

PREVIOUSLY there have been papers that dealt with laser device scaling with respect to weight, power, and pressure.¹⁻³ While there has also been a wealth of papers dealing with the propagation of laser beams through various media, the review paper by Gebhardt will suffice for the purposes of this work.⁴ This paper blends together two optimizations: 1) weight with respect to performance, and 2) power with respect to range in an effort to develop a rationale for selecting various laser systems candidates for the myriad of commercial and military applications.

System Weight Modeling

Chemical lasers are usually scaled to the first order by the overall performance parameters of specific power and nozzle power flux. These parameters are given the symbols S and δ , respectively, and the units of measure are given by their definitions, as follows:

S = power/mass flow rate, kJ/kg

δ = power/nozzle face area, kW/m^2

Presented at the AIAA/SD10 High-Power Laser Device Conference, Boulder, CO, March 2-5, 1987; received April 13, 1987; revision received Sept. 23, 1987. Copyright © American Institute of Aeronautics and Astronautics, Inc., 1988. All rights reserved.

*Visiting Lecturer, Department of Physics; currently at Doughty Research Engineering, Albuquerque, NM. Associate Fellow AIAA.

The performance parameters are used in the following manner to describe the weight of a chemical laser device:

$$W = F + BP_v/(n_x\delta) + CP_v t/(n_x S) + E(\delta/S) \quad (1)$$

The constants F , B , C , and E are determined from actual system designs. As weight models become more descriptive of the system, more terms are added to Eq. (1). However, for the purposes of this paper, we will retain the simple form.

For most HF/DF chemical lasers, the performance parameters, S and δ , have been determined from test data. The relationship of the two is shown in Fig. 1. The performance data for a particular dilution ratio Φ can be analytically represented by a parabola, of which we are only interested in the top half (real portion) of the curve.

$$S = [1 + (1 - \delta/\delta_m)^{1/2}]S_m/2 \quad (2)$$

Since the laser can be operated over a rather broad dilution ratio range, a representative parabola can be derived for each value of Φ ; then a curve can be fitted tangent to the set for all Φ , as shown in Fig. 2. The form of bounding performance curve is given by

$$S = K_1 \exp(-K_2\delta) \quad (3)$$

With analytic expressions relating S and δ , we can optimize the system weight with respect to a particular fixed Φ performance curve (a local optimum) and also the bounding performance curve (a global optimum). Consider a system without significant pressure recovery requirements, e.g., a space-based laser (SBL). The weight equation becomes a function of one variable. Rearranging, we get

$$W_1 = (W - F)n_x/P_v = B/\delta + Ct/f(\delta) \quad (4)$$

Substituting Eq. (2) for $f(\delta)$ and taking the derivative of W_1 , we can determine the performance that will minimize the weight.

$$\frac{(\delta/\delta_m)^2}{(1 - \delta/\delta_m)^{1/2}[1 + (1 - \delta/\delta_m)^{1/2}]^2} = \frac{B S_m}{Ct \delta_m} = Z^2 \quad (5)$$

Note that the optimum δ is a function of the laser device design parameters B & C and the system run time t . The magnitude of the weight scales directly with P_v/n_x . Equation (5) can be solved to determine δ_{OPT} in closed form by making a trigonometric substitution. The result is given below:

$$\delta_{opt}/\delta_m = -2Z^2 - Z^4/2 + (Z + Z^3/2)(Z^2 + 4)^{1/2} \quad (6)$$

S_{opt} is obtained from Eq. (2), and the minimum weight from Eq. (1). Similarly, we can derive the global optimum condition by substituting Eq. (3) for $f(\delta)$. The result is

$$\delta_{opt}^2 \exp(K_2\delta_{opt}) = BK_1/CtK_2 \quad (7)$$

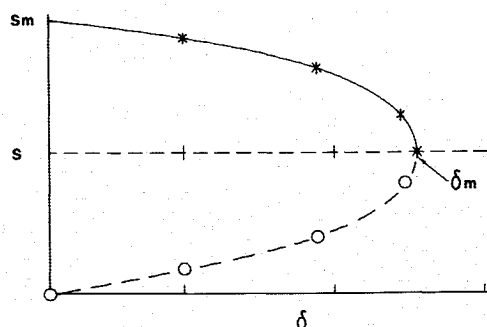


Fig. 1 Specific power-nozzle power flux relationship.

Examples of DF chemical laser optimization are shown in Fig. 3.

System weight models cover a spectrum of complexity, from the simple versions like Eq. (1) to sophisticated computer models that require hundreds of inputs and provide output information sufficient for the generation of preliminary conceptual design. For our purposes, the laser device can be represented by its major subsystems. The major chemical laser subsystems and their relation to system performance parameters are shown in Table 1. Note that $\delta/S = \dot{m}/A$, which is an important parameter in fluid dynamics. Let's now reconfigure Eq. (1) making use of \dot{m}/A .

$$W = F + P_v/n_x S[B/(\dot{m}/A) + Ct] + E(\dot{m}/A) \quad (8)$$

Using the perfect gas law and the definition of the Mach number,⁵ we can express \dot{m}/A in terms of the cavity pressure, temperature, and Mach number

$$\dot{m}/A = \rho V = P_c M \sqrt{k/R_g T_c} \quad (9)$$

By substituting Eq. (9) into Eq. (8), we now have the device weight as a function of Mach number in the optical cavity (resonator region):

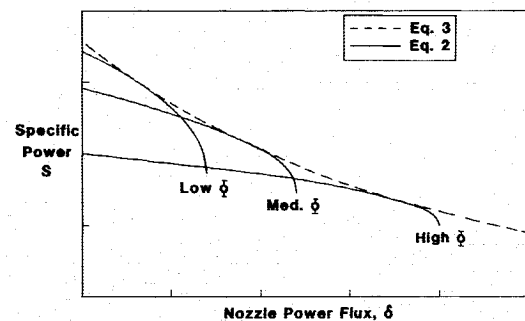


Fig. 2 Typical DF chemical laser performance variation with dilution ratio Φ .

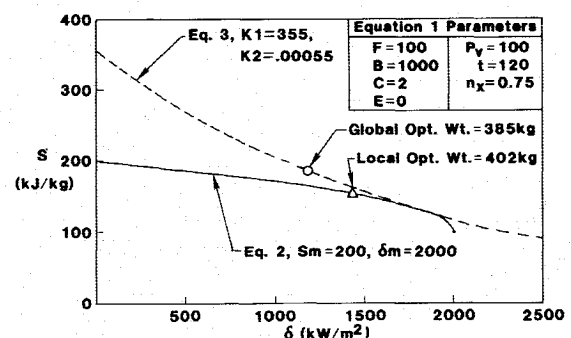


Fig. 3 System weight-performance optimization.

Table 1 Subsystem weight parameter dependency

Subsystem	Dependent factor
Laser and ejector fluid supply, <i>FSS</i>	$P_v t/n_x S$
Optical resonator, <i>ORS</i>	$P_v/n_x \delta$
Gain generator and diffuser, <i>GGG</i>	$P_v/n_x \delta$
Diffuser/ejector efficiency, $1.3 < M < 5$	δ/S
Control console, <i>CCS</i>	Fixed
Thermal management, <i>TMS</i>	$P_v/n_x S$
Oxygen generator, <i>OGS</i> (iodine laser only)	$P_v/n_x S$

$$W = F + P_v/n_x S[(B/p_c M)(R_g T_c/k)^{1/2} + Ct] + E p_c M(k/R_g T_c)^{1/2} \quad (10)$$

The Mach number dependency leads us to investigate supersonic flow devices as a means of reducing systems weight. Equation (10) is differentiated with respect to the Mach number; the minimum weight condition is shown by the dashed curve in Fig. 4. The solid curve is for a system without pressure recovery, e.g., an SBL.

Propagation

In this section, the laser beam generated by a minimum weight system is propagated along a horizontal path in the atmosphere to an object of interest. The irradiance equation for the focused beam peak intensity is

$$I_P = P_v T_A (1 - \epsilon^2) r_F^2 L_{TB} \exp[-(2\pi\phi)^2]/\pi R^2 \sigma^2 \quad (11)$$

Equation (11) is for a system that has a Gaussian illuminated output aperture. We can simplify Eq. (11) as follows:

$$I_P = P T_A L_{TB}/\pi R^2 \sigma^2 \quad (12)$$

where the power P is now that which emanates from the final output aperture so that we don't have to include wavefront error, mirror absorption, and obscuration losses in the formula. The atmospheric transmittance is given by

$$T_A = \exp(-\Gamma R) \quad (13)$$

where R is the range in kilometers. The atmospheric extinction coefficient Γ is equal to the sum of the molecular and aerosol contributions to absorption and scattering, respectively.

$$\Gamma = \alpha_m + \alpha_a + s_m + s_a \quad (14)$$

Molecular absorption values for DF in this paper are power weighted average using the MIRACL output spectrum.⁶ The molecular absorption values for iodine are also taken from Ref. 6 for the 3-4 hyperfine electronic transition. Molecular scattering for wavelengths greater than 1 μm is negligible.

The variation of the atmospheric extinction coefficient, coupled with other propagation phenomena, leads one quite naturally to search for the best laser wavelength for atmospheric propagation. Gebhardt concluded that the DF laser had the best overall transmission characteristics for a system without adaptive optics (AO). Recent advancements in adaptive optics

technology is causing a shift of the best wavelength towards the upper part of the visible spectrum for some scenarios.⁷

The laser beam spread consists of four major contributions: diffraction, pointing jitter, beam quality, and turbulence. Equations that describe these parameters are shown below:

Diffraction:

$$\sigma_D = \sqrt{2/\pi} (\lambda/D) \quad (15a)$$

Pointing:

$$\sigma_J = 2[\langle \theta_x^2 \rangle]^{1/2} \quad (15b)$$

Turbulence:

$$\sigma_t = 2.016 \lambda^{-1/5} (C_N^2 R)^{3/5} \quad (15c)$$

Total:

$$\sigma^2 = (\sigma_D^2 + \sigma_J^2)\beta^2 + \sigma_t^2 \quad (15d)$$

The beam quality β is a measure of the excellence of the beam, i.e., how close it approaches the theoretical limit of 1.0. The beam quality degradation affects both the diffractive and pointing jitter components of the total beam spread.⁸ Also, as will be shown, the jitter term will be taken as a certain fraction of the diffraction term so that the multiplication of both terms by β^2 , as in Eq. (15d), is proper. Beam qualities of 1.3 times diffraction limited have been measured for HF/DF chemical lasers. Values for β of 1.1 and better have been observed in some electric discharge pulse lasers. To assure good beam quality, device designers strive to provide laser optical media that are free of density gradients and mirrors with minimal figure distortion.

The diffraction term is for a focused Gaussian beam whose edge is defined by the $1/e$ point on the intensity profile.

The pointing jitter is described by the variance of the single axis jitter angle, which is assumed to be isotropic, and thus $\langle \theta_x^2 \rangle = \langle \theta_y^2 \rangle$. For best performance, the system pointing jitter should be about one-third the diffraction angle.⁹

$$\sigma_J = 0.33 \lambda/D \quad (16)$$

Terms in the turbulence induced beam spread equation [Eq. (15c)] contain the range (now in meters) and the atmospheric structure constant C_N^2 which is also referred to as the refractive index structure coefficient; C_N^2 varies with altitude, time of day, and geographic location. In order to make predictions of propagation and subsequent system performance, we must use a representative C_N^2 profile. Two versions are given here.

Modified Hufnagel¹⁰:

$$C_N^2 = 5.94(10^{-53})H^{10} \exp(-H/1000) + 2.7(10^{-16}) \times \exp(-H/1500) + 10^{-14} \exp(-H/100) \quad (17)$$

AFWL¹¹:

$$C_N^2 = 5(10^{-14})(H^{-0.8737}) \quad (18)$$

with linear spike at 10 km to peak at 11.2 km, where $C_N^2 = 4(10^{-17})$ with linear return to the curve at $H = 12,400$ m (12.4 km).

Before proceeding further, let's examine the irradiance equation in an expanded form.

$$I_P = \frac{P \exp[-(\alpha_m + s_m + \alpha_a + s_a)R] L_{TB}}{\pi R^2 \{[(0.45\lambda/D)^2 + (0.33\lambda/D)^2]\beta^2 + [2.016\lambda^{-1/5}(C_N^2 R)^{3/5}]^2\}} \quad (19)$$

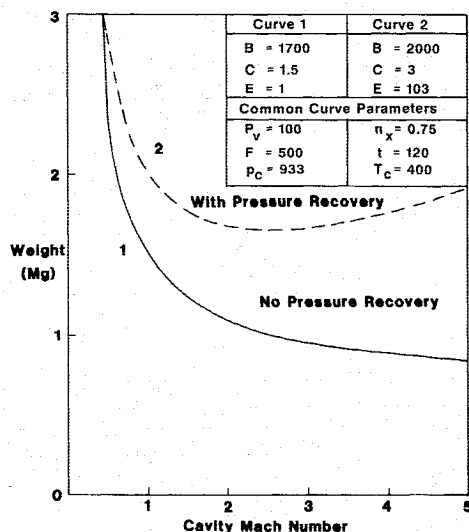


Fig. 4 System weight variation with Mach number.

We can see the nonlinear dependence of the intensity on λ , R , D , β , and C_N^2 , noting that absorption and scattering are also wavelength dependent. When the thermal blooming parameter L_{TB} is elaborated, additional nonlinearities become apparent.

$$L_{TB} = 1/(1 + 0.0625 N^2) \quad (20)$$

The thermal distortion parameter N is given by

$$N = \frac{-n_s(\alpha_m + \alpha_s)PR^2}{\pi n_0 \rho_0 C_P v_0 a_0^3} f_1(\Gamma R) f_2(a_0/G) f_3(w_s R/v_0) \quad (21)$$

where a_0 is the $1/e$ beam radius ($a_0 = D/2\sqrt{2}$), and the slew rate w_s is that of the beam relative to the transmitting aperture platform. The f_1 , f_2 , and f_3 functions relate to the finite attenuation, focusing, and slewing of the beam.

Now, with the inclusion of thermal blooming, more nonlinearity is explicitly introduced into the problem, e.g., P^2 , R^4 , and D^6 . Large complex optics codes have been constructed to examine in detail the propagation of the laser beam through the atmosphere accounting for the nonlinearities and physical property changes along the path.¹² If we remove thermal blooming from the problem by assuming sufficient clearing wind and/or modest beam intensities, a rather straightforward solution can be obtained for optimum propagation conditions. Note that such an assumption (removal of L_{TB}) is reasonable for systems incorporating adaptive optics, where it is assumed that the thermal blooming will be corrected to essentially the same level as the turbulence. Even systems without AO are assumed to be capable of correcting tilt and focus errors induced by turbulence.

Prior to developing a solution to Eq. (19), let us first lay additional foundation. Laser systems can be compared by their capability to deliver a required level of energy into a specified spot. Frequently, target material damage criteria are specified by the intensity at the edge of the damage spot and by the spot size. It is desired to minimize the total beam power while providing the required edge intensity. The peak intensity I_p is related to the edge intensity of a spot of radius r_s by

$$I_E = I_p \exp(-r_s^2/G^2) \quad (22)$$

where G is the Gaussian beam radius and is equal to $R\sigma$. It can be shown that the laser power is minimized when

$$I_E/I_p = e^{-1} \quad (23)$$

The relationship between the spot radius and the Gaussian beam is then

$$r_s = G = R\sigma \quad (24)$$

Since the total beam spread σ contains the turbulence contribution, which in turn has a nonlinear range dependency, Eq. (24) is most easily solved by iterating R , the range, using a calculator or microcomputer to any reasonable degree of accuracy (say 0.01 km). Note that the solution is that particular range, R_{opt} , at which the propagated beam delivers exactly the desired edge intensity at the required spot size. With the optimum range determined, the corresponding minimum power is then

$$P_{min} = I_E \pi (R_{opt} \sigma)^2 / [\exp(-\Gamma R_{opt}) - 1] \quad (25)$$

When the range is less than optimum, the beam can be dithered or defocused to spread it to fill the damage spot. The required power slightly decreases, since the transmission loss decreases with range. For $R < R_{opt}$

$$P = I_E \pi r_s^2 / [\exp(-\Gamma R) - 1] \quad (26)$$

For $R > R_{opt}$, the power must be increased to provide sufficient energy at the spot edge. Note that the actual beam, as defined by the $1/e$ intensity point, is now larger than the defined damage spot.

$$P = I_E \pi (R\sigma)^2 \exp[r_s^2/(R\sigma)^2] / \exp(-\Gamma R) \quad (27)$$

Solutions to Eqs. (25–27) can be obtained for laser systems at different wavelengths with and without AO, which can be explicitly included by selecting either the desired level of correction or the desired number of actuators to drive the deformable mirror surface. For a zonal AO correction scheme, the number of actuators is given by:¹³

$$N_A = [0.323/\ell \pi (1/SR)]^{6/5} (D/r_{CL})^2 \quad (28)$$

where SR is the Strehl ratio, which is defined as the actual peak intensity divided by the theoretical peak intensity, as if there were no atmospheric turbulence aberrations. The atmospheric correlation length r_{CL} is defined by

$$r_{CL} = 3.024 [C_N^2 R (2\pi/\lambda)^2]^{-3/5} \quad (29)$$

Sometimes it is desirable to know the Strehl ratio for a given number of actuators. Equation (28) can be combined with Eq. (29) to give

$$SR = \exp[-2.016 C_N^2 R \lambda^{-2} (D^2/N_A)^{5/6}] \quad (30)$$

For a system containing AO, the turbulence term is corrected such that the total beam spread σ becomes

$$\sigma^2 = (\sigma_D^2 + \sigma_J^2)\beta^2 + \sigma_D^2 (1/SR - 1) \quad (31)$$

The above system of equations can be solved for the optimum range and power for given input parameters for laser systems with and without AO. An example of such a solution set will now be given.

System Effectiveness

There is continuing interest throughout the laser technical community regarding the selection of the best laser for a given application. For very long range applications (> 100 km), the difference between peak and average intensity is insignificant for aperture sizes on the order of one meter. A measure of merit for comparing candidate systems is

$$M_1 = I_p/W \quad (32)$$

A measure of how effectively each unit of system weight is used to deliver the laser energy to an object is M_1 . For shorter range engagements where there is a significant difference between peak and average intensities over a specified spot, the following measure of merit is deemed more appropriate:

$$M_2 = I_E/W \quad (33)$$

Let us now compare two laser candidates for an airborne application. Conditions and assumptions common to both are given in Table 2 and the comparison results are shown in Fig. 5.

Table 2 Common system parameters

Beam quality, β	1.5	System pointing jitter, σ_J	1.25
Output aperture, D	1.0 m	Target spot radius, r_s	8.5
Aircraft altitude	12 km	DF atm. ext. coeff., Γ_{DF}	0.0021
Target altitude	12 km	I atm. ext. coeff., Γ_I	0.0016
Maximum range, R	60 km	Path C_N^2 , [$m^{-2/3}$]	$1.05(10^{-17})$
No. of actuators, N_A	61	Edge intensity, [W/cm ²]	50

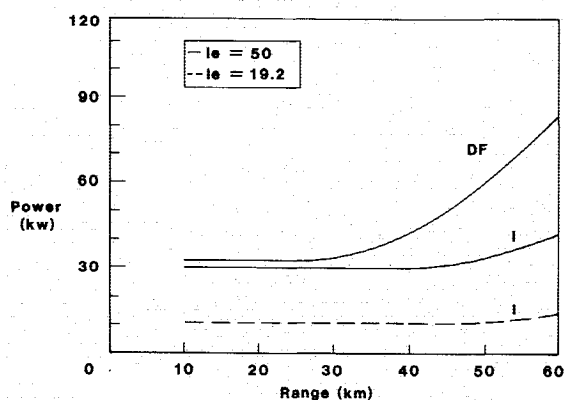


Fig. 5 Power vs range.

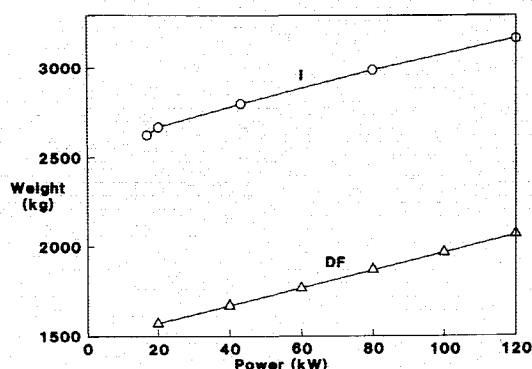


Fig. 6 Weight-power relations for DF and iodine systems.

When the target material is factored into the overall problem, there can be an advantage to the shorter wavelength laser. For targets made from fiberglass or graphite-epoxy materials, there is no significant wavelength sensitivity to irradiation. Metals do have a wavelength dependence. The coupling coefficient for aluminum can be expressed by

$$n_c = 0.2\lambda^{-0.9} \quad (34)$$

where λ is in μm . Thus, the coupling coefficients for DF and iodine, respectively, are 0.06 and 0.156. If the target is aluminum, the iodine laser power can consequently be reduced by a factor of 2.6, as shown by the dashed line in Fig. 5. The thermomechanical effects of materials subject to laser irradiation have recently been reported.¹⁴

Thermal blooming was insignificant ($L_{TB} = 0.9999$) for the example scenario because of the low power levels of the candidate systems, as well as other contributing factors.

Now let's determine the measure of merit for the two systems. The DF laser will be configured to operate in the high mass throughput (\dot{m}/A) regime, so that an auxiliary ejector will not be required. The iodine laser must operate at very low cavity pressure and will, therefore, require a single stage ejector to exhaust the laser gas to the ambient pressure at the 12 km altitude. By the substitution of the appropriate values into Eq. (1), we can generate weight curves as shown in Fig. 6. Taking the values for weight at the maximum required power points for DF and iodine results in the following:

DF:

$$M_2 = 50/1870 = 0.027W/\text{kg} - \text{cm}^2$$

Iodine:

$$M_2 = 50/2800 = 0.018W/\text{kg} - \text{cm}^2$$

For a metallic (aluminum) target, the measures of merit are now dependent on the equivalent incident edge intensity, but the iodine system weight is decreased due to lower power resulting from better coupling.

DF:

$$M_2 = 50/1870 = 0.027W/\text{kg} - \text{cm}^2$$

Iodine:

$$M_2 = 50/2620 = 0.019W/\text{kg} - \text{cm}^2$$

For these conditions and assumptions, the DF system having a measure of merit better than the iodine system would be selected. However, a different decision might be made at higher power levels. For example, the weight curves for the DF and iodine lasers cross in the vicinity of 2 MW. For a similar set of requirements as discussed above, other factors such as device volume and cost would have to be included to reach an equitable decision (assuming, of course, that weight curves are still accurate after an order of magnitude scale-up in power). If the mirror surface finish and system pointing accuracy can be improved to take full advantage of the better diffractive properties of the shorter wavelengths, then these factors will also have an impact on the selected system.

Conclusions

Following the procedures outlined in this paper, one can determine optimum ranges and powers for candidate laser systems in ground, air, naval, and space scenarios. For fixed ground based lasers, the most appropriate measure of merit is system cost, which in turn is predominantly a function of the device efficiency and the atmospheric transmission of its corresponding wavelength. One searches for the wavelength that is the best combination of overall propagation properties, coupling coefficient, if there is a metallic target, and mirror performance. Space laser system selection is strongly driven by minimum weight on orbit, which implies M_1 as the appropriate comparator.

The work described in this paper is currently being extended to include integration algorithms for slant path propagation, as well as models for pulsed chemical laser weight, propagation, and target coupling.

Acknowledgments

I would like to acknowledge the support and encouragement for this work from my students and Dr. S. Rosenwaks of the Physics Department of Ben-Gurion University. Mr. Y. Tzuk determined the closed form solution to Eq. (5). Mr. R. Acebal, Dr. F. G. Gebhardt, and Dr. L. Zajac provided many helpful comments.

References

- Wilson, L. E. and Doughty, J. R., "Scaling of DF and HF Chemical Lasers for Air Force Missions (U)," *Proceedings of the First Department of Defense Conference on HEL Technology*, Vol. 3, Dec. 1974, p. 185.
- Forbes, S. G., Trost, J. E., Ackerman, R. A., and Clendening, C. W., "Long Range Chemical Laser Program," Air Force Weapons Laboratory, Kirtland Air Force Base, NM, AFWL-TR-77-144, March 1978, p. 23.
- Quan, V. and Dickerson, R. A., "Pressure-Geometry Scaling for Chemical Laser Performance," *AIAA Journal*, Vol. 23, July 1985, pp. 1133-1135.

⁴Gebhardt, F. G., "High Power Laser Propagation," *Applied Optics*, Vol. 15, June 1976, pp. 1479-1493.

⁵Shapiro, A. H., *The Dynamics and Thermodynamics of Compressible Fluid Flow*, Vol. I, Ronald Press, New York, 1953, pp. 84-87.

⁶Leslie, D. H., "Altitude-Dependent Atmospheric Absorption of DF, HF, and Iodine Laser Radiation," NRL Memorandum Rept. 4906, Sept. 28, 1982.

⁷Boye, C. A. and Hogge, C. B., "Wavelength Dependence of Adaptive Optics Compensation," SPIE Proceedings, Vol. 410, April 1983, pp. 161-173.

⁸Radley, J., General Research Corp., private communication, Dec. 1979.

⁹Negro, J. E., "HEL Applications Study (U)," Air Force Weapons Laboratory, Kirtland Air Force Base, NM, AFWL-TR-78-250, Vol. 2, Annex T6, Nov. 1978, p. 15.

¹⁰Butts, R. R. and Hogge, C. B., "Point-Ahead Limitation on Adaptive Optics for Ground to Space Transmission," Air Force Weapons Laboratory, Kirtland Air Force Base, NM, AFWL-TR-79-46, 1979, p. 65.

¹¹Airborne Laser Engineering (ABLE) Phase 2 Additional Mission and Technology Information, SAIC, Albuquerque, NM, July 1983 (Algorithm from AFWL).

¹²Novoseller, D., TRW Defense Systems Group, private communication, Dec. 1983.

¹³Pearson, J. E., "Adaptive Optics: A State-of-the-Art Report," *Laser Focus*, Sept. 1981, pp. 53-61.

¹⁴Chang, C. I., Griffis, C. A., Stonesifer, F. R., and Nemes, J. A., "Thermomechanical Effects of Intense Thermal Heating on Materials/Structures," *Journal of Thermophysics and Heat Transfer*, Vol. 1, April 1987, pp. 175-181.

*Recommended Reading from the AIAA
Progress in Astronautics and Aeronautics Series . . .*



Opportunities for Academic Research in a Low-Gravity Environment

George A. Hazelrigg and Joseph M. Reynolds, editors

The space environment provides unique characteristics for the conduct of scientific and engineering research. This text covers research in low-gravity environments and in vacuum down to 10^{-15} Torr; high resolution measurements of critical phenomena such as the lambda transition in helium; tests for the equivalence principle between gravitational and inertial mass; techniques for growing crystals in space—melt, float-zone, solution, and vapor growth—such as electro-optical and biological (protein) crystals; metals and alloys in low gravity; levitation methods and containerless processing in low gravity, including flame propagation and extinction, radiative ignition, and heterogeneous processing in auto-ignition; and the disciplines of fluid dynamics, over a wide range of topics—transport phenomena, large-scale fluid dynamic modeling, and surface-tension phenomena. Addressed mainly to research engineers and applied scientists, the book advances new ideas for scientific research, and it reviews facilities and current tests.

TO ORDER: Write AIAA Order Department,
370 L'Enfant Promenade, S.W., Washington, DC 20024

Please include postage and handling fee of \$4.50 with all orders.
California and D.C. residents must add 6% sales tax. All foreign orders
must be prepaid. Please allow 4-6 weeks for delivery. Prices are subject
to change without notice.

1986 340 pp., illus. Hardback
ISBN 0-930403-18-5
AIAA Members \$59.95
Nonmembers \$84.95
Order Number V-108